 CMES, vol.30, no.1, pp.17-26, 2008

An Efficient Model for Crack Propagation

S.S. Xu and Y. Dong and Y. Zhang

Abstract: A meshless method for arbitrary crack growths is presented. The new method is based on a local partition of unity by introducing additional degrees of freedom that determine the opening of the crack. The crack is modeled with overlapping crack segments located at the nodes. The crack segments are rotated at directional changes of the principal tensile stress such that smearing of the crack is avoided. Such smearing occurs in fixed crack method probably because of inaccurate stress state around the crack tip when the crack propagates. The key feature of our method is that it does not require algorithms to track the crack path. The simplicity of our method makes it is especially useful for industrial applications.

Keyword: meshless, crack, enrichment, fracture

1 Introduction

Reliability and life assessment analysis is important in many industrial applications. Nowadays, numerical methods are often exploited for such task. Especially critical is the assessment of structures that contain cracks and flaws. The simulation of cracking still remains a challenge in numerical methods. Smeared crack methods were the focus of research especially in the 80s and 90s, Zimmermann (1986); Bazant and Oh (1983); Jirasek and Zimmermann (1998); Malvar and Fourney (1990). They can be classified into fixed and rotating cracks. The latter models were developed since one found that fixed crack models gave too stiff responses. Meshless methods have proven to be a powerful alternative in simulating arbitrary growing cracks, Belytschko, Lu, and Gu (1994a); Belytschko and Lu (1995); Belytschko, Lu, and Gu (1995); Hao, Liu, Klein, and Rosakis (2004); Li and Simonson (2003); Han and Atluri (2003); Tang, Shen, and Atluri (2003); Liu, Han, Rajendran, and Atluri (2006); Nairn (2003); Guo and Nairn (2004); Liu, Hao, and Belytschko (1999); Hao, Liu, and Chang (2000); Rabczuk and Belytschko (2005); Rabczuk, Belytschko, and Xiao (2004); Hao and Liu (2006). They were applied to modelling static crack growth in 2D for non-linear materials Hagihara, Tsunori, and Ikeda (2007); Nishioka, Kobayashi, and Fujimoto (2007); Fujimoto and Nishioka (2006); Chandra and Shet (2004), piezo-electric materials Sladek, Sladek, and Zhang (2007); Nguyen-Van, Mai-Duy, and Tran-Cong (2008) including temperature effects Chen, Gan, and Chen (2008) and contact Guz, Menshykov, and Zozulya (2007) in continua and structures Rabczuk and Areias (2006); Andreaus, Batra, and Porfiri (2005); Rabczuk, Areias, and Belytschko (2007). There are also few papers on three-dimensional crack growths Krysl and Belytschko (1999); Guo and Nairn (2006); Sladek, Sladek, and Krivacek (2005); Rabczuk and Belytschko (2007); Rabczuk, Bordas, and Zi (2007), dynamic fracture Maiti and Geubelle (2004); Guz, Menshykov, and Zozulya (2007); Gao, Liu, and Liu (2006); Andreaus, Batra, and Porfiri (2005); Le, Mai-Duy, and Tran-Cong (2008) and multiscale cracking Ma, Lu, and Wang (2006) using meshless methods. An excellent overview of state-of-the-art numerical techniques for fracture can be found in Nishioka (2005).

Meshless methods were pioneered by Atluri and Zhu (1998, 2000); Atluri and Shen (2002), Belytschko, Lu, and Gu (1994b); Belytschko and Tabbara (1996); Belytschko, Krongauz, Organ, Fleming, and Krysl (1996), Liu, Jun, and Zhang (1995) and other, see e.g. Duarte and Oden (1996); Melenk and Babuska (1996). They offer the opportunity to model the crack explicitly. Due to the absence of a mesh, the crack can propagate

arbitrarily. The visibility criterion Belytschko, Lu, and Gu (1994a) and modifications such as the transparency and diffraction method are used to model the correct kinematics of the crack. An excellent book about meshless methods, their applications and abilities is given in Atluri (2002).

In linear elastic fracture mechanics, the singularity dominates the stress field around the crack tip. Stress intensity factors or the energy release rate is used as failure criterion. However, linear elastic fracture mechanics is only applicable to very brittle materials. If nonlinear material behavior is to be modeled, different approaches have to be used. Cohesive zone models Barenblatt (1962); Hillerborg, Modeer, and Peterson (1976) are commonly used to describe the post-localization behavior. This is necessary for materials with strain softening since the use of pure continuum models lead to mesh dependent results Bazant and Belytschko (1985).

One key issue in discrete crack models is how to track the crack path. This is especially cumbersome for large numbers of cracks and in three dimensions.

We present a cohesive crack method that bridges smeared crack models with discrete meshless crack methods. These type of methods are especially suitable for many cracks and three-dimensional crack growths. Remmers, deBorst, and Needleman (2003) were the first who proposed such a cohesive segment method. In their approach, they introduced disconnected cohesive segments within finite element method similar to the well known extended finite element method. Similar methods in finite element concept were developed by Sancho, Planas, and Fathy (2007); Feist and Hofstetter (2007). Rabczuk and Belytschko (2004) developed the cracking particle method in meshfree method. This method is based on a local partition of unity where the crack is modeled by discrete crack segments through a node. Hence, there is no need for tracking the crack path. In their paper, they used a fixed crack approach and their results show spurious cracking and over-smearing of crack width. Based on the approach in Rabczuk and Belytschko (2004), we propose a rotating crack method that avoids this over-smearing. The crack orientation at initiation is determined by the Rankine criterion.

2 Meshless shape functions and displacement field

Meshless methods are based only on nodal approximations. The elementfree Galerkin approximation (EFG) Belytschko, Lu, and Gu (1994b) is based on a partition of unity concept Rabczuk and Zi (2007). The partition of unity concept is especially useful in the context of material failure since the kinematics of the crack can be incorporated elegantly into the formulation. Therefore, the approximation of the displacement field is decomposed into a continuous $\mathbf{u}^{con}$ and discontinuous part $\mathbf{u}^{dis}$:

$$\mathbf{u}(\mathbf{x}) = \mathbf{u}^{con}(\mathbf{x}) + \mathbf{u}^{dis}(\mathbf{x}) \tag{1}$$

The continuous EFG shape functions are calculated by a moving least square approximation, where the approximation is written in terms of a polynomial basis $\mathbf{p}(\mathbf{x})$ and unknown coefficients $\mathbf{a}(\mathbf{x})$:

$$\mathbf{u}^h(\mathbf{x}) = \sum_i p_i(\mathbf{x})\, a_i(\mathbf{x}) = \mathbf{P}^T(\mathbf{x})\, \mathbf{a}(\mathbf{x}) \tag{2}$$

Commonly, a linear basis $\mathbf{p}^T(\mathbf{x}) = (1, x, y)$ is used. Minimizing a discrete weighted $\mathscr{L}_2$ error norm with respect to the unknown coefficients $\mathbf{a}$

$$J = \sum_I \left(\mathbf{P}^T(\mathbf{x}_I)\, \mathbf{a}(\mathbf{x}_I) - \mathbf{u}_I\right)^2 w(\mathbf{x} - \mathbf{x}_I, h) \tag{3}$$

where $w(\mathbf{x} - \mathbf{x}_I, h)$ is a so-called weighting function and h determines the interpolation radius of the weighting function, leads finally to the famous EFG approximation

$$\mathbf{u}^{con}(\mathbf{x}) = \sum_{I \in \mathscr{W}} N_I(\mathbf{x}) \mathbf{u}_I \tag{4}$$

with the EFG shape functions

$$N_I(\mathbf{x}) = \mathbf{p}^T(\mathbf{x})\, A^{-1}(\mathbf{x})\, \mathbf{D}_I(\mathbf{x}) \tag{5}$$

and

$$\begin{aligned} \mathbf{D}_I(\mathbf{x}) &= w(\mathbf{x} - \mathbf{x}_I, h) \mathbf{p}^T(\mathbf{x}_I) \\ \mathbf{A}_I(\mathbf{x}) &= \sum_I w(\mathbf{x} - \mathbf{x}_I, h)\, \mathbf{p}(\mathbf{x}_I)\, \mathbf{p}^T(\mathbf{x}_I) \end{aligned} \tag{6}$$

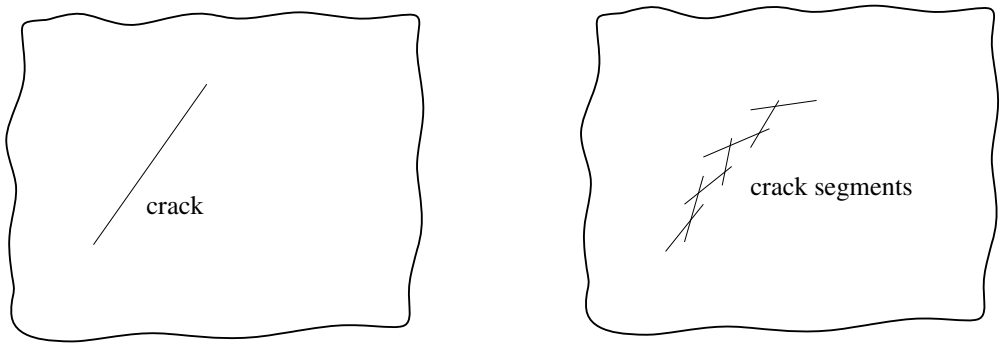

Figure 1: Crack and representation of the crack with overlapping discrete cohesive crack segments

We propose to model the discrete crack by overlapping cohesive crack segments that pass through the node instead of trying to create a continuous crack surface, figure 1. This circumvents the need of tracking the crack path. The crack kinematics is obtained by the discontinuous displacement approximation that is active only for nodes that contain the cohesive crack segments:

$$\mathbf{u}^{dis}(\mathbf{x}) = \sum_{I \in \mathscr{W}_c} N_I(\mathbf{x})\ \Psi(\mathbf{x})\ \mathbf{q}_I \tag{7}$$

where $\mathscr{W}_c$ are the nodes where the cohesive crack segments pass through, $\mathbf{q}_I$ are additional unknowns and $\Psi(\mathbf{x})$ is the enrichment function describing the crack kinematics. A common enrichment function that is able to capture the correct crack kinematics is the step function

$$\Psi(\mathbf{x}) = \begin{cases} 1 & \text{if } \mathbf{n}\cdot(\mathbf{x}-\mathbf{x}_I) > 0 \\ -1 & \text{if } \mathbf{n}\cdot(\mathbf{x}-\mathbf{x}_I) < 0 \end{cases} \tag{8}$$

Note that only cracked nodes are enriched. The length of the cohesive segment is equal to the size of the domain of influence of the associated cracked node. The jump in the displacement field $[[\mathbf{u}]] = \mathbf{u}^{\Omega_+} - \mathbf{u}^{\Omega_-}$, where the subscript of Ω indicates the different sides of the crack, only depends on the additional degrees of freedom $\mathbf{q}_I$:

$$[[\mathbf{u}]](\mathbf{x}) = \sum_{I \in \mathscr{W}_c} 2\ N_I(\mathbf{x})\ \mathbf{q}_I \tag{9}$$

We used the Rankine criterion to generate a crack. The orientation of the crack is perpendicular to the direction of the maximum principal stress. Since the stress around the crack tip is inaccurate especially at crack initiation, we use a rotating crack segment approach where the crack segments are rotated according to directional changes in the maximum principal stress. We will show by numerical examples that over-smearing of the crack occurs when the orientation of the crack is fixed. We believe that the initial inaccuracies of the stress field around the crack tip at crack initiation cause this crack smearing.

The discrete strain field can be derived as

$$\nabla \mathbf{u}^s(\mathbf{x}) = \sum_{I \in \mathscr{W}} \nabla N_I(\mathbf{x})\ \mathbf{u}_I + \sum_{I \in \mathscr{W}_c} \nabla N_I(\mathbf{x})\ \Psi(\mathbf{x})\ \mathbf{q}_I \tag{10}$$

Integration is done using Gauss quadrature.

3 The cohesive law

In the cohesive model, the traction is related to the crack opening, equation (9):

$$t_n = f_t - \frac{f_t}{\delta_{max}}[[u]]_n \text{if} [[u]]_n < \delta_{max} \text{ and } [[u]]_n^{t+\Delta t} > [[u]]_n^t$$
$$\text{otherwise } t_n = 0 \text{ when } [[u]]_n^{t+\Delta t} > [[u]]_n^t \tag{11}$$

where

$$[[u]]_n = \mathbf{n}\cdot[[\mathbf{u}]] \tag{12}$$

is the crack opening and δ_{max} is the point where the traction have decayed to zero. Unloading is linear elastic.

Due to its simplicity, we employed the Rankine criterion where the crack is inserted once the maximum principal tensile stress exceeds the tensile strength.

4 Equilibrium equations and discretization

The equation of equilibrium for a geometrically linear system is:

$$\begin{aligned} \nabla \cdot \mathbf{P} + \mathbf{b} &= \mathbf{0}\ \mathbf{x} \in \Omega && (13)\\ \mathbf{u} &= \bar{\mathbf{u}}\ \mathbf{x} \in \Gamma_u && (14)\\ \mathbf{n}_t \cdot \mathbf{P} &= \bar{\mathbf{t}}\ \mathbf{x} \in \Gamma_t && (15)\\ \mathbf{n}_c \cdot \mathbf{P} &= \mathbf{t}_c([[\mathbf{u}]])\ \mathbf{x} \in \Gamma_c && (16) \end{aligned}$$

where $\mathbf{u}$ are the displacements, $\mathbf{t}$ are the tractions, $\mathbf{P}$ is the stress tensor, $\mathbf{b}$ are the body forces, Γ is the boundary and the subscript u, t, c denote "displacement", "traction" and "crack", respectively. With the test functions $\mathbf{v}$ that are of similar structure than the trial functions, equations (4), (7), the weak form of the equations of equilibrium can be assembled:

$$\sum_{j=1}^{n} \left[\int_{\Omega_j} \nabla^s \mathbf{v}_j : \mathbf{P}\, d\Omega + \int_{\Gamma_{c,j}} \mathbf{v} \cdot \mathbf{t}_c\, d\Gamma \right] = \sum_{j=1}^{n} \int_{\Gamma_{t,j}} \mathbf{v} \cdot \bar{\mathbf{t}}\, d\Gamma \quad (17)$$

Inserting the trial functions, equations (7) and (4), and the test functions that are of similar structure into equation (18), the equation to be solved is given in matrix form:

$$\int_{\Omega} \hat{\mathbf{B}}^T\ \mathbf{P}\, d\Omega + \int_{\Gamma_c} \hat{\mathbf{N}}^T \mathbf{t}_c\, d\Gamma = \int_{\Gamma_t} \hat{\mathbf{N}}^T \bar{\mathbf{t}}\, d\Gamma + \int_{\Omega} \hat{\mathbf{N}}^T \mathbf{b}\, d\Omega \quad (18)$$

where $\hat{\mathbf{B}}$ and $\hat{\mathbf{N}}$ contain continuous and discontinuous shape functions and their spatial derivatives, respectively. Continuous B-matrix:

$$\mathbf{B}_I^u = \begin{bmatrix} N_{I,x} & 0 \\ 0 & N_{I,y} \\ N_{I,y} & N_{I,x} \end{bmatrix} \quad (19)$$

Discontinuous B-matrix:

$$\mathbf{B}_I^q = \begin{bmatrix} \tilde{N}_{I,x} & 0 \\ 0 & \tilde{N}_{I,y} \\ \tilde{N}_{I,y} & \tilde{N}_{I,x} \end{bmatrix} \quad (20)$$

with $\tilde{N} = N\Psi(\mathbf{x})$.

The final system of equations:

$$\begin{bmatrix} \mathbf{K}_{IJ}^{uu} & \mathbf{K}_{IJ}^{uq} \\ \mathbf{K}_{IJ}^{qu} & \mathbf{K}_{IJ}^{qq} \end{bmatrix} \cdot \begin{bmatrix} \Delta \mathbf{u}_J \\ \Delta \mathbf{q}_J \end{bmatrix} = \begin{bmatrix} \mathbf{f}_{I,ext}^{u} - \mathbf{f}_{I,int}^{u} \\ \mathbf{f}_{I,ext}^{q} - \mathbf{f}_{I,int}^{q} \end{bmatrix} \quad (21)$$

is solved with an incremental iteration scheme in which

$$\mathbf{K}_{IJ}^{ij} = \int_{\Omega} \left(\mathbf{B}_I^i\right)^T\ \mathbf{C}\, \mathbf{B}_J^j\, d\Omega + \kappa \int_{\Gamma_c} \mathbf{N}^T\, \mathbf{D}\, \mathbf{N}\, d\Gamma \quad (22)$$

where $\kappa = 1$ when $i = j = q$, otherwise $\kappa = 0$, $\mathbf{D}$ is the tangential stiffness of the cohesive model and the superscript i and j indicate u and q for the continuous and discontinuous shape functions and

$$\mathbf{f}_{I,ext}^{i} = \int_{\Gamma_t} \left(\mathbf{N}_I^i\right)^T\ \mathbf{t} d\Gamma + \int_{\Omega} \left(\mathbf{N}_I^i\right)^T\ \mathbf{b} d\Omega \quad (23)$$

$$\mathbf{f}_{I,int}^{i} = \int_{\Omega} \left(\mathbf{B}_I^i\right)^T\ \mathbf{P} d\Omega + \int_{\Gamma_c} \left(\mathbf{N}_I^q\right)^T\ \mathbf{t}_c d\Gamma \quad (24)$$

5 Results

Three examples are tested. The first example, specimen under uni-axial tension, is academic example to verify the method. It can be used as simple benchmark problem for other researchers to test novel methods. The second example is a notched two-point bending sample and the last example is a three-point bending beam that develops several cracks.

5.1 Uni-axial tensile test

A simple mode I failure is studied first. The system is depicted in Figure 2. The square plate is fixed at the bottom and is loaded a the top edges with uniform displacement boundary conditions. A horizontal pre-crack exists on the left-hand side of the structure. The material has a Young's modulus $E = 100$ and Poisson's ration $\nu = 0.0$, tensile strength $f_t = 0.05$ and fracture energy $G_f = 0.01$. We study this problem with different number of nodes and show results for 400 nodes and 1,600 nodes. Our aim is to prove that the results (load-displacement curve) is independent of the number of degrees of freedom. This control has to be done for any new numerical method.

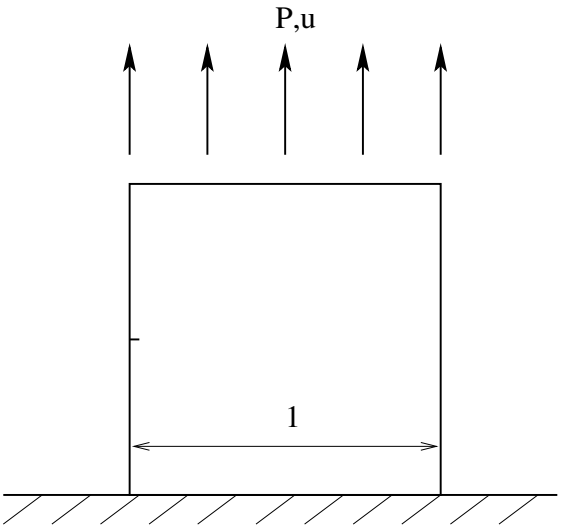

Figure 2: Square plate subject to uni-axial tension

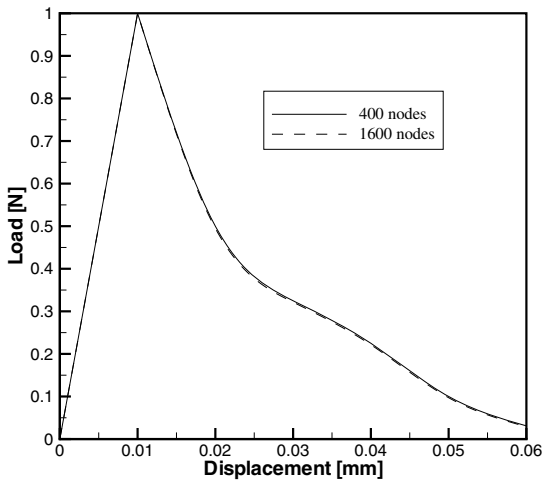

Figure 3: Load-displacement curve of the uni-axial tensile test

The crack begins to propagate from the pre-notch perpendicular to the direction the load is applied. The crack is perfectly straight as expected and not illustrated. The load-displacement for 400 nodes and 1,600 nodes is presented in figure 3. The load-displacement curve is independent of the number of nodes.

5.2 Tensile-shear beam

As a second example, the pre-notched beam in figure 4 is subjected by two concentrated forces F. The beam has a rectangular cross-section with thickness 156mm. The material has a Young's modulus $E = 25,000$MPa, Poisson's ratio $\nu = 0.2$, tensile strength $f_t = 2.8$MPa and fracture energy $G_f = 100$N/m. This experiment was done by Arrea and Ingraffea (1982).

The crack propagates from the prenotch obliquely. Initially shear stresses dominate the crack orientation. In the later stage, dominant tensile stresses cause the crack to straighten. Figure 5 shows the crack pattern for the rotating vs. fixed crack method. The crack is smeared wider for the fixed crack method probably due to inaccuracies in the crack orientation at initiation. The crack pattern of the rotating crack method is closer to the experimental data of Arrea and Ingraffea (1982).

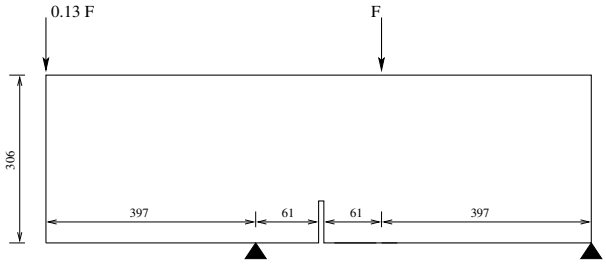

Figure 4: The prentoch beam subject to two concentrated loads; all dimensions are in mm

(a) Fixed crack method

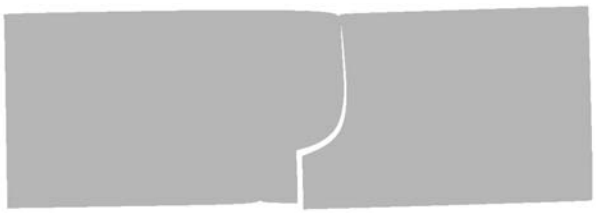

(b) Rotating crack method

Figure 5: Crack in the tensile-shear beam

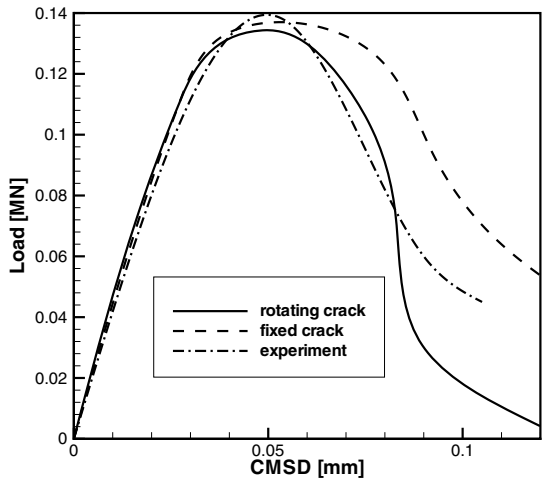

Figure 6: Load vs. crack mouth sliding displacement

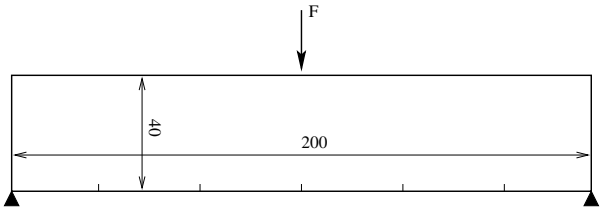

Figure 7: 3-point beam in bending

Also the load-displacement curve is stiffer for the fixed crack method, figure 6. It overestimates the fracture energy and falls outside the experimental data. Note that the experimental data underlies certain scatter in the post-localization. We show the averaged curve. The rotating crack method is closer to the experimental data except close to the end of the load-displacement curve but experimental measurements are difficult when the beam is close to fracture.

5.3 3-point bending beam

The final example is 3-point beam in bending. The geometry and dimensions of the beam are depicted in figure 7. The material has a Young's modulus $E = 36{,}000$MPa, Poisson's ratio $\nu = 0.2$, tensile strength $f_t = 3$MPa and fracture energy $G_f = 100$N/m. Initially, bending stresses are dominant at crack initiation at the bottom and cracks propagate perpendicular to the bottom line. The cracks incline due to shear stresses at a later stage. Figure 8 shows that the fixed crack method smears the crack widely and is less realistic than the rotating crack method.

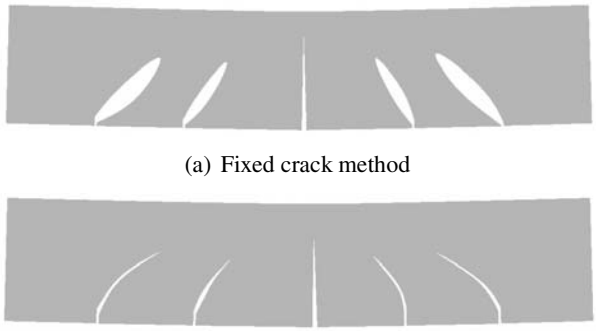

(a) Fixed crack method

(b) Rotating crack method

Figure 8: Cracks in the 3-point bending beam

6 Conclusions

The discrete rotating cohesive crack method was implemented into a meshfree concept. In this method, the crack was modelled by a set of cracked cohesive segments that directly pass through the nodes. The partition of unity method was exploited to describe the crack kinematics. The Rankine criterion initiated the crack at the node and the crack segment was placed perpendicular to the direction of the maximum principal tensile stress though other criteria such as the strong-ellipticity criterion can be used. The discrete crack segments were allowed to rotate if directional changes in the principal tensile stresses occur. Since the stress field is especially inaccurate around the crack tip, this strategy improves the results and avoids smearing of the cracks that is observed when the crack orientation is fixed at initiation. The method is applied to three examples and shows good behavior.

The proposed method could also be employed for a dynamic analysis. It is especially effective for many cracks and complicated crack pattern that includes fragmentation. These applications will be investigated in our future research.

References

Andreaus, U.; Batra, B.; Porfiri, M. (2005): Vibrations of cracked euler-bernoulli beams using meshless local petrov-galerkin (mlpg) method. *CMES: Computer Modeling in Engineering & Sciences*, vol. 9, pp. 111–131.

Arrea, M.; Ingraffea, A. (1982): Mixed mode crack propagation in mortar and concrete. *Cornell University, Department fo Structural Engineering*, , no. 81-13.

Atluri, S. (2002): *The Meshless Local Petrov-Galerkin (MLPG) Method*. Tech Science Press.

Atluri, S.; Shen, S. (2002): The meshless local petrov-galerkin method: a simple and less-costly alternative to the finite element and boundary element methods. *Computations and Modelling in Engineering and Sciences*, vol. 3, pp. 11–51.

Atluri, S.; Zhu, T. (1998): A new meshless local petrov-galerkin (mlpg) approach in computational mechanics. *Computational Mechanics*, vol. 22, pp. 117–127.

Atluri, S.; Zhu, T. (2000): The meshless local petrov-galerkin (mlpg) approach for solving problems in elasto-statics. *Computational Mechanics*, vol. 25, pp. 169–179.

Barenblatt, G. (1962): The mathematical theory of equilibrium of cracks in brittle fracture. *Advances in Applied Fracture*, vol. 7, pp. 55–129.

Bazant, Z.; Belytschko, T. (1985): Wave propagation in a strain softening bar: exact solution. *Journal of Engineering Mechanics ASCE*, vol. 11, pp. 381–389.

Bazant, Z.; Oh, B. (1983): Crack band theory for fracture in concrete. *Materials and Structures*, vol. 16, pp. 155–177.

Belytschko, T.; Krongauz, Y.; Organ, D.; Fleming, M.; Krysl, P. (1996): Meshless methods: An overview and recent developments. *Computer Methods in Applied Mechanics and Engineering*, vol. 139, pp. 3–47.

Belytschko, T.; Lu, Y. (1995): Element-free galerkin methods for static and dynamic fracture. *International Journal of Solids and Structures*, vol. 32, pp. 2547–2570.

Belytschko, T.; Lu, Y.; Gu, L. (1994): Crack propagation by element-free galkerin methods. *Engineering Fracture Mechanics*, vol. 51, pp. 295–315.

Belytschko, T.; Lu, Y.; Gu, L. (1994): Element-free galerkin methods. *International Journal for Numerical Methods in Engineering*, vol. 37, pp. 229–256.

Belytschko, T.; Lu, Y.; Gu, L. (1995): Crack propagation by element-free galerkin methods. *Engineering Fracture Mechanics*, vol. 51, no. 2, pp. 295–315.

Belytschko, T.; Tabbara, M. (1996): Dynamic fracture using element-free galerkin methods. *International Journal for Numerical Methods in Engineering*, vol. 39, no. 6, pp. 923–938.

Chandra, N.; Shet, C. (2004): A micromechanistic perspective of cohesive zone approach in modeling fracture. *CMES: Computer Modeling in Engineering & Sciences*, vol. 5, no. 1, pp. 21–33.

Chen, Z.; Gan, Y.; Chen, J. (2008): A coupled thermo-mechanical model for simulating the material failure evolution due to localized heating. *CMES: Computer Modeling in Engineering & Sciences*, vol. 26, no. 2, pp. 123–137.

Duarte, C.; Oden, J. (1996): An h-p adaptive method using clouds. *Computer Methods in Applied Mechanics and Engineering*, vol. 139, pp. 237–262.

Feist, C.; Hofstetter, G. (2007): 3D fracture simulations based on the sda. *International Journal for Numerical and Analytical Methods in Geomechanics*, vol. 31, pp. 189–212.

Fujimoto, T.; Nishioka, T. (2006): Numerical simulation of dynamic elasto visco-plastic fracture using moving finite element method. *CMES: Computer Modeling in Engineering & Sciences*, vol. 11, no. 2, pp. 91–101.

Gao, L.; Liu, K.; Liu, Y. (2006): Applications of mlpg method in dynamic fracture problems. *CMES: Computer Modeling in Engineering & Sciences*, vol. 12, no. 3, pp. 181–195.

Guo, Y.; Nairn, J. (2004): Calculation of j-integral and stress intensity factors using the material point method. *CMES: Computer Modeling in Engineering & Sciences*, vol. 6, no. 3, pp. 295–308.

Guo, Y.; Nairn, J. (2006): Three-dimensional dynamic fracture analysis using the material point method. *CMES: Computer Modeling in Engineering & Sciences*, vol. 16, no. 3, pp. 141–155.

Guz, A.; Menshykov, O.; Zozulya, V. (2007): Contact problem for the flat elliptical crack under normally incident shear wave. *CMES: Computer Modeling in Engineering & Sciences*, vol. 17, no. 3, pp. 205–214.

Hagihara, S.; Tsunori, M.; Ikeda, T. (2007): Application of meshfree method to elastic-plastic fracture mechanics parameter analysis. *CMES: Computer Modeling in Engineering & Sciences*, vol. 17, no. 2, pp. 63–72.

Han, Z.; Atluri, S. (2003): Truly meshless local petrov-galerkin (mlpg) solutions of traction and displacement bies. *Computations and Modelling in Engineering and Sciences*, vol. 4, pp. 665–678.

Hao, S.; Liu, W. (2006): Moving particle finite element method with superconvergence: Nodal integration formulation and applications. *Computer Methods in Applied Mechanics and Engineering*, vol. 195, no. 44-47, pp. 6059–6072.

Hao, S.; Liu, W.; Chang, C. (2000): Computer implementation of damage models by finite element and meshfree methods. *Computer Methods in Applied Mechanics and Engineering*, vol. 187, no. 3-4, pp. 401–440.

Hao, s.; Liu, W.; Klein, P.; Rosakis, A. (2004): Modeling and simulation of intersonic crack growth. *International Journal of Solids and Structures*, vol. 41, no. 7, pp. 1773–1799.

Hillerborg, A.; Modeer, M.; Peterson, P. E. (1976): Analysis of crack formation and crack growth in concrete by means of fracture mechanics and finite elements. *Cement and Concrete Research*, vol. 6, pp. 773–782.

Jirasek, M.; Zimmermann, T. (1998): Analysis of rotating crack model. *Journal of Engineering Mechanics*, vol. 124, pp. 842–851.

Krysl, P.; Belytschko, T. (1999): The efgm for dynamic propagation of arbitrary three-dimensional cracks. *International Journal for Numerical Methods in Engineering*, vol. 44, no. 6, pp. 767–800.

Le, P.; Mai-Duy, N.; Tran-Cong, T. (2008): A meshless modeling of dynamic strain localization in quasi-brittle materials using radial basis function networks. *CMES: Computer Modeling in Engineering & Sciences*, vol. 25, no. 1, pp. 43–67.

Li, S.; Simonson, B. C. (2003): Meshfree simulation of ductile crack propagation. *International Journal of Computational Methods in Engineering Science and Mechanics*, vol. 6, pp. 1–19.

Liu, H.; Han, Z.; Rajendran, A.; Atluri, S. (2006): Computational modeling of impact response with the rg damage model and the meshless local petrov-galerkin (mlpg) approaches. *Computers Materials and Continua*, vol. 4, pp. 43–53.

Liu, W.; Hao, S.; Belytschko, T. (1999): Multiple scale meshfree methods for damage fracture and localization. *Computational Material Science*, vol. 16, no. 1-4, pp. 197–205.

Liu, W.; Jun, S.; Zhang, Y. (1995): Reproducing kernel particle methods. *International Journal for Numerical Methods in Engineering*, vol. 20, pp. 1081–1106.

Ma, J.; Lu, H.; Wang, B. (2006): Multiscale simulation using generalized interpolation material point (gimp) method and molecular dynamics (md). *CMES: Computer Modeling in Engineering & Sciences*, vol. 14, no. 2, pp. 101–117.

Maiti, S.; Geubelle, P. (2004): Mesoscale modeling of dynamic fracture of ceramic materials. *CMES: Computer Modeling in Engineering & Sciences*, vol. 5, no. 2, pp. 91–101.

Malvar, L.; Fourney, M. (1990): A three dimensional application of the smeared crack approach. *Engineering Fracture Mechanics*, vol. 35, no. 1-3, pp. 251–260.

Melenk, J.; Babuska, I. (1996): The partition of unity finite element method: Basic theory and applications. *Computer Methods in Applied Mechanics and Engineering*, vol. 139, pp. 289–314.

Nairn, J. (2003): Material point method calculations with explicit cracks. *CMES: Computer Modeling in Engineering & Sciences*, vol. 4, no. 6, pp. 649–663.

Nguyen-Van, H.; Mai-Duy, N.; Tran-Cong, T. (2008): A smoothed four-node piezoelectric element for analysis of two-dimensional smart structures. *CMES: Computer Modeling in Engineering & Sciences*, vol. 23, no. 3, pp. 209–222.

Nishioka, T. (2005): Recent advances in numerical simulation technologies for various dynamic fracture phenomena. *CMES: Computer Modeling in Engineering & Sciences*, vol. 10, no. 3, pp. 209–215.

Nishioka, T.; Kobayashi, Y.; Fujimoto, T. (2007): The moving finite element method based on delaunay automatic triangulation for fracture path prediction simulations in nonlinear elastic-plastic materials. *CMES: Computer Modeling in Engineering & Sciences*, vol. 17, no. 3, pp. 231–238.

Rabczuk, T.; Areias, P. (2006): A meshfree thin shell for arbitrary evolving cracks based on an extrinsic basis. *CMES: Computer Modeling in Engineering & Sciences*, vol. 16, no. 2, pp. 115–130.

Rabczuk, T.; Areias, P.; Belytschko, T. (2007): A meshfree thin shell method for non-linear dynamic fracture. *International Journal for Numerical Methods in Engineering*, vol. 72, no. 5, pp. 524–548.

Rabczuk, T.; Belytschko, T. (2004): Cracking particles: A simplified meshfree method for arbitrary evolving cracks. *International Journal for Numerical Methods in Engineering*, vol. 61, no. 13, pp. 2316–2343.

Rabczuk, T.; Belytschko, T. (2005): Adaptivity for structured meshfree particle methods in 2d and 3d. *International Journal for Numerical Methods in Engineering*, vol. 63, no. 11, pp. 1559–1582.

Rabczuk, T.; Belytschko, T. (2007): A three-dimensional large deformation meshfree method for arbitrary evolving cracks. *Computer Methods in Applied Mechanics and Engineering*, vol. 196, no. 29-30, pp. 2777–2799.

Rabczuk, T.; Belytschko, T.; Xiao, S. (2004): Stable particle methods based on lagrangian kernels. *Computer Methods in Applied Mechanics and Engineering*, vol. 193, pp. 1035–1063.

Rabczuk, T.; Bordas, S.; Zi, G. (2007): A three-dimensional meshfree method for continuous multiple-crack initiation, propagation and junction in statics and dynamics. *Computational Mechanics*, vol. 40, no. 3, pp. 473–495.

Rabczuk, T.; Zi, G. (2007): A meshfree method based on the local partition of unity for cohesive cracks. *Computational Mechanics*, vol. 39, no. 6, pp. 743–760.

Remmers, J.; deBorst, R.; Needleman, A. (2003): A cohesive segments method for the simulation of crack growth. *Computational Mechanics*, vol. 31, no. 69-77.

Sancho, J.; Planas, J.; Fathy, A. (2007): 3D simulation of concrete fracture using embedded crack elements without enforcing crack path continuity. *International Journal for Numerical and Analytical Methods in Geomechanics*, vol. 31, pp. 173–187.

Sladek, J.; Sladek, V.; Krivacek, J. (2005): Meshless local petrov-galerkin method for stress and crack analysis in 3-d axisymmetric fgm bodies. *CMES: Computer Modeling in Engineering & Sciences*, vol. 8, no. 3, pp. 259–270.

Sladek, J.; Sladek, V.; Zhang, C. (2007): Fracture analyses in continuously nonhomogeneous piezoelectric solids by the mlpg. *CMES: Computer Modeling in Engineering & Sciences*, vol. 19, no. 3, pp. 247–262.

Tang, Z.; Shen, S.; Atluri, N. (2003): Analysis of materials with strain-gradient effects: A meshless local petrov-galerkin(mlpg) approach, with nodal displacements only. *Computations and Modelling in Engineering and Sciences*, vol. 4, pp. 177–196.

Zimmermann, T. (1986): Failure and fracturing analysis of concrete structures. *Nuclear Engineering and Design*, vol. 92, no. 3, pp. 389–410.